A Hybrid FDM-BIEM Approach for Earthquake Dynamic Rupture Simulation

N. Kame[1], H. Aochi[2]
[1]*Kyushu University, Fukuoka, Japan;* [2]*BRGM, Orleans, France*

1. Introduction.

There have been proposed many numerical methods to simulate dynamic shear crack growth in an elastic medium, which is a model of earthquake faulting in seismology. Such numerical studies began in the 1960's and we are still seeking more precise methods. The difficulty comes from the existence of discontinuity, shear crack(s), in a continuum body. It always generates a kind of singularity that is hard to evaluate numerically and spurious oscillations thus tend to occur in the solutions.

A boundary integral equation method (BIEM) has been a powerful tool in such crack problems. The advantage is in the relatively small resources required in computation because the problem is solved not in the whole volume, but only on the crack interfaces. In most cases, BIEM is formulated in an infinite homogeneous elastic medium for which the Green function can be derived in an analytic form [1,2]. It is because the stress kernels of BIEM consist of the analytic Green function, which guarantees the accuracy of the kernels. Consequently BIEM is accurate in such homogeneous cases, but not applicable to arbitrary inhomogeneous medium. In order to compensate this inconvenience, some numerical efforts have been studied recently [3,4], and we make a further step towards this direction.

For this purpose, we here newly develop a hybrid method using BIEM and a finite difference method (FDM), hereafter we call " Hybrid finite Difference-Boundary integral equation Method (HDBM)". This is an extension of BIEM to an arbitrary inhomogeneous medium with the facilitative use of FDM in evaluating the stress kernels numerically.

2. Method

(2.1) Boundary Integral Equation Method (BIEM) as our starting point

In a linear elastic medium we consider, the displacement field anywhere can be written in the form of convolution over the origin of deformation, which is now the discontinuity on the interface Σ without any external forces. This is known as a representation theorem,

$$u_n(\boldsymbol{x}) = \int_{-\infty}^{\infty} d\tau \int_{\Sigma} \Delta u_i c_{ijpq} \nu_j \frac{\partial}{\partial \xi_q} G_{np}(\boldsymbol{x}, t-\tau; \boldsymbol{\xi}, 0) d\Sigma, \qquad \text{(Eq.1)}$$

where ν is a normal vector on the interface Σ, G_{np} is the Green function of the medium, representing the *n*-th displacement component for an impulse force in the *p*-direction and the summation rule is taken for the repeated subscripts on the right hand side. BIEM is based on its derivative form, namely the stress

expression in terms of the slip on the fault, after renormalizing hypersingularity appeared in the derivative of the Green function [5,6,7,8].

In the case of an infinite, homogeneous medium, the analytical expression of the Green function is available for (Eq.1) so that the boundary integral equation for the stress field on the interface can be written down. The mathematical formulation is quite long to show here but well summarized in [8]. For the discretization, it is often used to divide the interface with equally spaced elements and with time step equally taken. Then a constant, uniform slip-rate, $d\Delta u/dt$, is given on an element of a length Δs during a time step Δt and the evaluation of stress is carried out on the center of the element at the end of the time step. The stress on the *I*-th element at the *K*-th time step is written in a very simple formulation using the discretized slip-rate $V^{I:K}$,

$$\tau^{I:K} = -\frac{\mu}{2V_S} V^{I:K} + \sum_{L} \sum_{N=0}^{K-1} P^{I-L;K-N} V^{L:N} , \qquad \text{(Eq.2)}$$

where on the right hand side, the first term is the instantaneous term and the second one is the contribution from the past history, being *P* the stress kernel of BIEM, which has the spatial and temporal symmetry. Here the time step is taken as

$$\Delta t = \frac{\Delta s}{2V_P} . \qquad \text{(Eq.3)}$$

Note that a longer time step than this does not allow the isolation of the instantaneous term like (Eq. 2), which clearly indicates the instantaneous response of $V^{I:K}$, to the stress drop in $\tau^{I:K}$.

(2.2) Hybrid finite Difference-Boundary integral equation Method (HDBM)

We here aim to replace the BIEM stress kernel $P^{I:K}$ in (Eq.2) by the one numerically evaluated using FDM. Similar method has been proposed in [3] for simulating the rupture dynamic in a heterogeneous medium, in which the numerical kernel in it is calculated and its deviation to the one in a homogeneous medium is appended in the BIEM framework. However in their framework, the numerical kernels are canceled out in a homogeneous medium so that the technique is not verified in a homogeneous medium. Therefore, we calculate all the kernels numerically so that we are able to verify our method in a simple homogeneous case. The calculated kernels are stocked for the later HDBM simulations. It is to be noted that this can be expensive for a complex problem that does not have any spatial symmetry in the kernels.

First we examine in detail the FDM evaluated kernel that is to be used in the later HDBM simulations. We consider mode II deformation in an infinite homogeneous medium with the density ρ=3000[kg/m^3], the P-wave velocity V_P=5480[m/s], and the S-wave velocity V_S=3164[m/s]. The situation we test is as follows. A unit element of a length Δs_{BIEM} corresponding to the BIEM is located at the origin in (x_1,x_2) coordinate. Writing exactly, this element is embedded between (-50[m], 0[m]) and (50[m], 0[m]) within a time step Δt_{BIEM} between

0[sec] and 0.0091[sec] ($\Delta t_{BIEM} = \Delta s_{BIEM} / 2V_P$). A kinematic source of a unit velocity on the BIEM element is given in the form of equivalent moment release rate $-\frac{dM_0}{dt}/\Delta s^3$ by adding to the FDM shear grids, where M_0 is the released moment on the BIEM element.

With regard to FDM, we here adopt the second-order staggered grid [9]. A kinematic source of a unit slip velocity on a fault element corresponding to a unit BIEM element size and time step is equivalently replaced in the form of released moment release rate by adding $-(dM_0/dt)/\Delta s^3$ on the FDM shear component grids [10]. As the unit source defined in the BIEM is a piece-wise both in space and in time (highly rapid change) and FDM calculation is inevitably accompanied with numerical oscillations in high frequencies. Note that, as the number of points per wavelength is required 10 in the second order FDM, the frequency limit is estimated as $f_{\max} = V_{min}/10\Delta s$, where V_{min} is the lowest velocity of the medium if inhomogeneity is considered. The FDM grids corresponding the unit source element just include the edge points at x_1= -50[m] and 50[m]. According to the BIEM framework, the evaluation point of stress value is located at $i \times \Delta s_{BIEM}$ on x_2 axis and at time $(k+1) \times \Delta t_{BIEM}$, letting i and k zero or positive integer numbers.

Fig.1 shows raw results of FDM calculation with four different resolutions Δs_{FDM} for this configuration. The sharp signal can be reproduced as the FDM grids are finer and the stress field at a long time is also well reproduced in its amplitude. As the supposed type of the unit source is discontinuous in space and time, high frequency oscillations are significant as we expected. Thus it requires some technique to remove them.

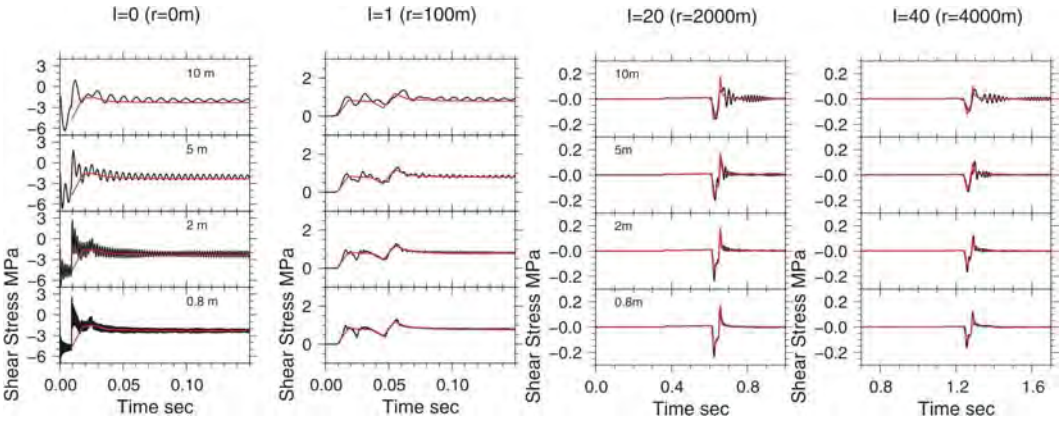

(Fig.1) Raw simulation results of FDM for calculating the numerical kernels. The grid spacing of FDM simulations is 10, 5, 2 and 0.8 m and time step is 0.5[ms], 0.25[ms], 0.01[ms] and 0.004[ms], respectively. Four positions are at x_1 = 0, 100, 2000 and 4000[m]. Red lines represent the analytical solutions (BIEM kernels) with a time step of Δt_{BIEM} = 0.0091[s].

Our collocation point (stress evaluation point) of the BIEM is chosen at the center of each element and at the end of each time step, and the discretization is strictly based on the P-wave velocity V_P. This means that the causality before and after the collocation points is different especially when the P-wave arrives (see time Δt_{BIEM} = 0.0091[s] in the first two panels in Fig.1). This is why we do not apply any filter in frequency domain. Instead, we adopt an averaging filter before each collocation point in time domain. Thus

$$P_{FDM}^{I:K} = ave(\tau(x = I\Delta s_{BIEM}),t);\ t = [(K + co)\Delta t : (K + 1)\Delta t], \qquad \text{(Eq.4)}$$

where we change the value of *co*, theoretically between 0 and 1. In the case of *co = 1*, no smoothing is applied and the value at $t = (K + 1)\Delta t$ is instantaneously used. We first try *co*=0.99 for different FDM resolutions and then take mixed values *co*=0.99 and 0.95, or *co*=0.99 and *co*=0.9 for the finest resolution as stated in Fig.2.

In order to seek an optimum *co* value, we consider the spatial summations of the kernels at each time step $\Sigma_I P^{I:K}$. Fig.2 shows the time series in a short (left) and a long (right) time ranges. Analytically this quantity must be zero except for *K=0*, where the instantaneous term $P^{0:0}$ only appears, and can thus be used as a checkpoint for the FDM kernels. It is observed that the convergence is sufficiently good for the finest grid Δs_{FDM} = *0.8*[m] (Fig.2, left). In the later time steps, each curve shows larger fluctuation (Fig.2, right). This is due to the reflected waves from the FDM model boundary, although we impose a strict absorbing condition [11] at all the boundaries. These reflected waves are not so visible in the time series of the kernels, but clearly seen in the summations and they must affect the results of longer duration simulations.

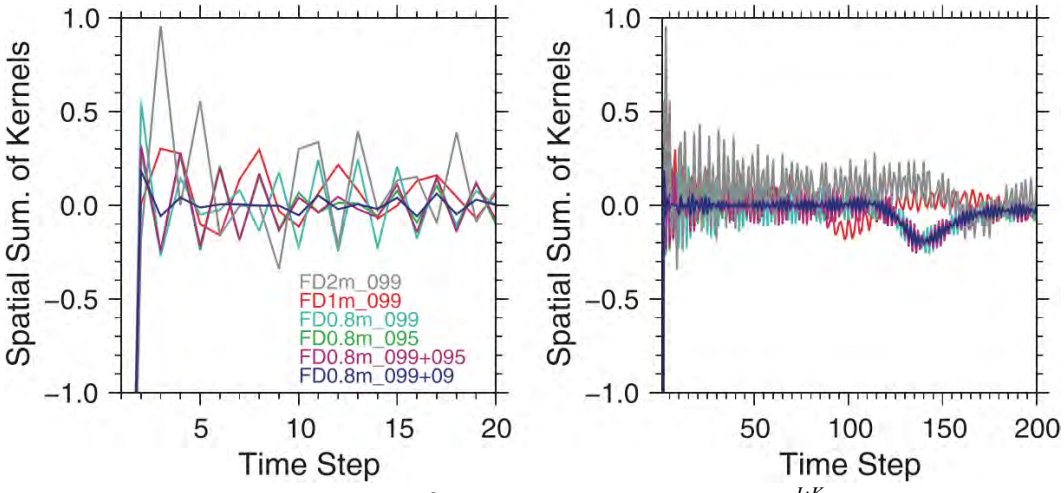

(Fig. 2) The spatial summation of the numerical kernels ($\Sigma_I P^{I:K}$) at each time step *K* [FD2m_099, FD1m_099, FD0.8m_099]. The first three colors curves are created by *co=0.99* for different FDM resolutions, Δs_{FDM} = *2*, *1*, and *0.8*[m]. [FD0.8m_095] *co= 0.95* for Δs_{FDM} does not improve a lot. [FD0.8m_099+095,

FD0.8m_099+09] The last two curves apply *co=0.95* and *0.9* for the kernel at origin (*I = 0*) while *co=0.99* for the others ($I \neq 0$).

In order to improve our results, we try to reduce the oscillations on the numerical kernels without losing any physical signals. When we take *co=0.95*, but the result is not significantly better. This is especially because the kernel on the origin (*I = 0*) is oscillated more than the others. Then we apply *co=0.95* or *0.9* only for the element of *I=0*, while we keep *co=0.99* for other kernels ($I \neq 0$). This procedure provides a quite good result and we finally choose optimum *co* values as stated below. The checkpoint we adopted is helpful to judge the quality of the FDM calculation. When we in future extend FDM calculation for a case of heterogeneous medium where $\Sigma_I P^{I:K}$ is not necessarily zero, we employ the optimum *co* for this homogeneous case.

Fig.3 compares the analytical (BIEM) and the numerical (FDM) kernels. The latter will be used in the later HDBM simulations. With respect to the unit source of BIEM (a duration of 0.0091[sec] = 110[Hz]), $f_{\max}$ is 396[Hz] for the Δs=80[m] of FDM. Through preliminary experiences above, the numerical kernels are finally obtained after smoothing the raw FDM calculations during the last one percent of the BIEM time step. The residual is less than 10% of signals including the adjacent and on-source elements. Main difference appears around the wave fronts, where the FDM suffers the numerical dissipations, however the amplitude of signals and the residual stress are evaluated correctly. To conserve the quantity $\Sigma P^{I:K}$ equal to zero is satisfactory.

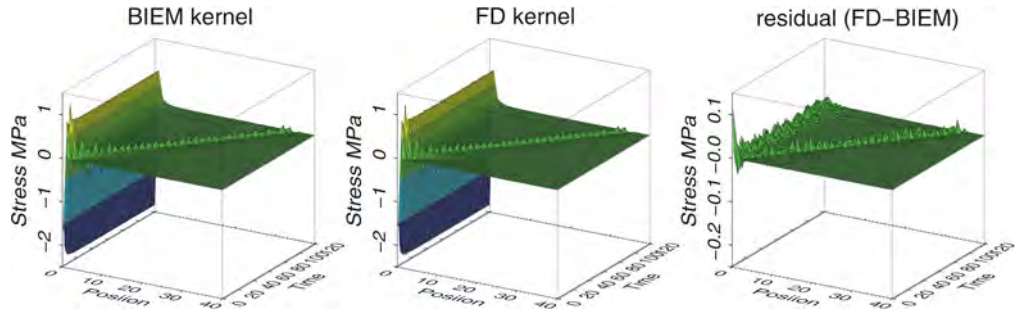

(Fig.3) Comparison of the analytical (BIEM) and numerical (FDM) kernels. A unit source is given at the origin. Both axes are shown in grid Δs and in time step Δt. In physical unit, Δs=100[m], Δt= 0.009[s] and V_P=5.48[km/s]. The grid spacing and time step of the FDM calculation are taken as 0.8[m] and 0.04[ms]. This kernel corresponds to FD0.8m_099+09.

3. Test Problem: Spontaneous Rupture Propagation

We test our HDBM with a simple test problem where an initiated crack propagates spontaneously on a planar fault and validate how fine FDM grids are sufficient to HDBM. In order to describe spontaneous rupture, we employ a slip-weakening law [12],

$$\sigma(\Delta u) = T_p - \Delta\tau(1-\Delta u/D_c)H(1-\Delta u/D_c), \qquad \text{(Eq.5)}$$

where the breakdown strength drop $\Delta\tau$ is defined as $\Delta\tau \equiv T_p - T_r$, being T_p and T_r peak strength and residual strength, respectively. $H(\cdot)$ is the Heaviside step function, and the parameter D_c is called as critical slip displacement, which is considered to control the scaling behavior in earthquake. This relation is graphically shown in (Fig.4a) and the given initial condition and the model parameters are shown in (Fig.4b). In this study, the effect of normal stress does not play a role because we consider a plane fault.

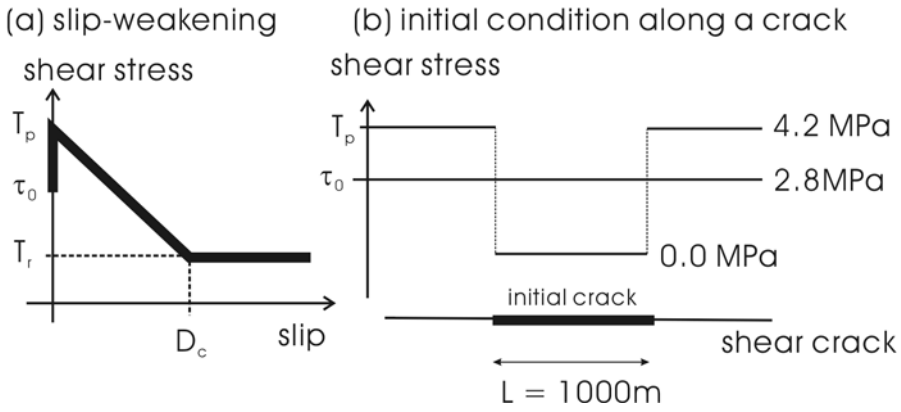

(Fig.4) (a) Constitutive relation between shear stress and slip defined by the slip-weakening law, (Eq.5). (b) Initial condition along a crack: initial crack length L=1000[m], initial shear stress τ_0=2.8[MPa], strength in the initial crack T_p=0.0[MPa], strength outside the initial crack T_p=4.2[MPa], residual strength T_r=0.0[MPa], and critical slip displacement D_c=0.1[m]. On the initial crack L, given shear stress exceeds the yielding stress T_p.

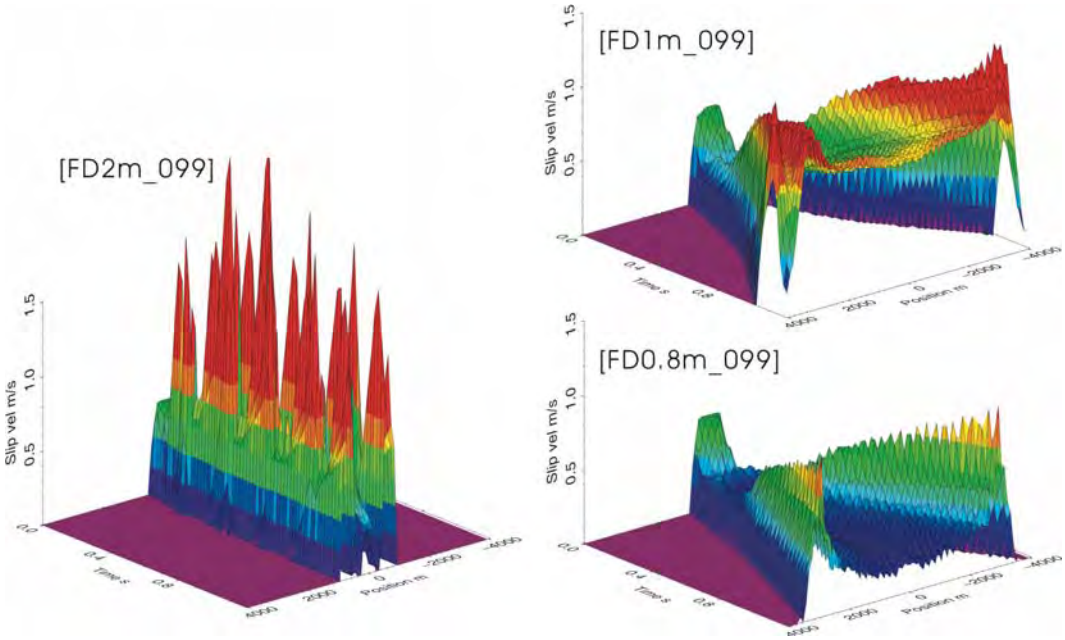

(Fig.5) HDBM simulation results for the test problem using three different FDM kernels with grid sizes, 2[m], 1[m], 0.8[m]. Filtering parameter is chosen to *co*=0.99. Graphics are smoothed every 0.02 second along the time axis

Fig.5 shows the simulation results using three numerical kernels for the test problem. As expected, the convergence of the cases $\Delta s_{FDM} = 2$[m] and 1[m] is not enough to obtain the correct solution. Regardless of the perturbation of the kernel with $\Delta s_{FDM} = 0.8$[m], we can obtain qualitatively good results in terms of the rupture velocity and peak slip rate. It is found that the required FD resolution is a hundred times finer for a basic element of the BIEM, and this is reasonable from the viewpoint of the maximum frequency that the FD scheme can reproduce (Fig.1) as pointed out above.

In addition, we made a further effort, smoothing the kernel applying spatially different *co* parameters, to extract more suitable discrete kernels. Finally a better result comparable to BIEM is simulated using the kernel with 0.8[m] grid smoothed over a 1% of time step before each collocation time point at origin except a 10% for the rest element [FD0.8m_099+09] (Fig.6). Compared with the [FD0.8m_099] result in Fig.5, the velocity peak with a sharp form moving with the rupture front propagation is reproduced better by the [FD0.8m_099+09] result. Both BIEM and HDBM include more of oscillations as the integral domain becomes larger in space and in time, but the global behaviors of rupture propagation are kept consistent.

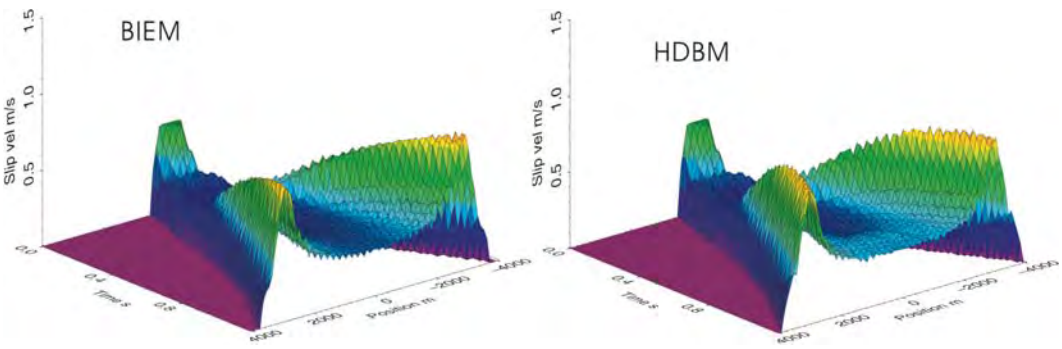

(Fig.6). Simulation results for spontaneous rupture propagation by BIEM and HDBM with the best kernel. Graphics are smoothed every 0.02 second along the time axis.

4. Summary

We proposed a hybrid method in which the stress kernels of BIEM are evaluated numerically by using FDM and named it “Hybrid finite Difference Boundary integral equation Method (HDBM)”. It is aimed to simulate a spontaneous earthquake rupture process in an inhomogeneous medium. We first asserted its validity in a homogeneous medium though HDBM is principally applicable for any inhomogeneity. We found that FDM calculation needs about 100 times finer

grids for a corresponding analytic BIEM kernel and that some additional smoothing in time series are also useful in the improvement of the FDM kernel. We then confirmed that our approach works sufficiently for a simple problem of mode II rupture propagation on a planar fault. Dynamic rupture growth in the presence of structural heterogeneity is to be investigated in future.

5. References

[1] K. Aki, P. Richards, Quantitative Seismology (2nd ed), University Science Books, New York, (2002), pp.565-590.

[2] M. Bouchon, F. J. Sanchez-Sesma, Boundary integral equations and boundary elements methods in elastodynamics. Advances in Geophysics (48) (2007) 157-189

[3] H. Goto, L. Ramirez-Guzman, J. Bielak, Numerical simulation of dynamic fault rupture propagation based on a combination of BIEM and FEM solutions, 14th WCEE Proceedings (2008), Beijing, China.

[4] K. B. Olsen, E. Fukuyama, H. Aochi, R. Madariaga, Hybrid modeling of curved fault radiation in a 3D heterogeneous medium, 2nd ACES Workshop Proceedings (2000), Brisbane, Australia.

[5] A. Cochard A, R. Madariaga, Dynamic faulting under rate-dependent friction. Pure appl. Geophys. (142) (1994) 419—445

[6] N. Kame, T. Yamashita, Simulation of the spontaneous growth of a dynamic crack without constraints on the crack tip path, Geophys. J. Int. (139) (1999) 345-358

[7] H. Aochi, E. Fukuyama, M. Matsu'ura, Spontaneous rupture propagation on a non-planar fault in 3-D elastic medium, Pure appl. Geophys. (157) (2000) 2003-2027

[8] T. Tada T, R. Madariaga, Dynamic modelling of the flat 2-D crack by a semi-analytic BIEM scheme. Int. J. numer. Mech. Engng. (50) (2001) 227-251

[9] J. Virieux, R. Madariaga, Dynamic faulting studied by a finite difference method, Bull. Seism. Soc. Am. (72) (1982) 345-369

[10] K.B. Olsen, Simulation of three-dimensional wave propagation in the Salt Lake Basin, PhD Thesis, pp157, University of Utah, Salt Lake City

[11] D. Komatitsch, R. Martin, An unsplite convolutional perfectly matched layer improuved at grazing incidence for the seismic wave equation, Geophysics (72) (2007) SM155-167

[12] Y. Ida, Cohesive force across the tip of a longitudinal-shear crack and Griffith's speciic surface energy, J. Geophys. Res. (77) (1972), 3796-3805